Supporting Information

Roberts et al. 10.1073/pnas.1215696110

SI Materials and Methods

Generation of *Smg1*$^{+/gt}$ Mice, Animal Husbandry, and Genotyping from RNA. The loss-of-function mutation in *Smg1* was produced by Genetrap mutagenesis in ES cells supplied by mutant mouse regional resource centers (MMRRC) (SIGTR ES cell line AG0297). The Genetrap cassette was randomly inserted into intron 4 of the murine *Smg1*. The cassette contains a strong splice acceptor site, β-galactosidase, and neomycin resistance genes, as well as multiple stop codons in each reading frame. The ES cells were injected into SV129 blastocysts to generate chimeric mice, crossed with C57BL/6 mice to generate *Smg1*$^{+/gt}$ mice. All animal experiments were approved by the Animal Ethics Committee at the Queensland Institute of Medical Research (QIMR). Mating was assumed at midnight and timed from 0.5 dpc. The genotype of each mouse was confirmed by reverse transcriptase PCR. RNA was isolated from mouse tails at postnatal day 10 using Trireagent (Sigma), and cDNA was generated using SuperScript III (Invitrogen). Each PCR assay comprised a final concentration of 1× reaction buffer (Invitrogen), 2 mM $MgCl_2$, dNTPs, 0.5 μM forward primers, 0.5 μM reverse primers, AmpliTaq Gold (Invitrogen), 250 ng of cDNA, and distilled water to 20 μL. Sequences of the primers used are as follows: forward primers for *Smg1* WT allele 5′ GCT CCT CTA CTT GTG TGC C 3′, reverse primer for *Smg1* WT allele 5′ TGA GGG TAG CAA CGA GCC 3′, forward primers for Genetrap cassette 5′ CGA AGA CTG GCT ACT GTA AAG C 3′, and reverse primers for Genetrap cassette 5′ GTA ATG GGA TAG GTC ACG TTG GTG 3′. PCR conditions begin with initial denaturation and activation of Taq polymerase at 95 °C for 10 min, followed by 35 cycles of denaturation at 95 °C for 30 s, annealing at 55 °C for 30 s, extension at 72 °C for 1 min, and a final extension at 72 °C for 10 min. WT *Smg1* allele generated a 190-bp product, whereas the Genetrap cassette generated a 450-bp product.

Genotyping Embryos. Genotyping of embryonic day (E) 6.5 to E8.5 embryos was performed by quantitative RT-PCR analysis. E6.5 to E8.5 embryos were isolated, and RNA was obtained using an RNeasy micro kit (QIAGEN) according to the manufacturer's instructions. cDNA was made using SuperScript III according to the manufacturer's instructions. Each PCR assay comprised a final concentration of 1× SYBR Master Mix (Applied Biosystems), 0.8 μM forward and reverse primers, 10 ng of cDNA, and distilled water to 20 μL. Primer sequences are shown in Table S3. PCR conditions begin with initial denaturation and activation of Taq at 95 °C for 10 min, followed by 50 cycles at 95 °C for 15 s and 60 °C for 1 min, and end with dissociation. All samples were run on an ABI 7900 sequence detection system with SDS version 1.9 software (Applied Biosystems). Mice that were *Smg1*$^{+/gt}$ showed a 50% reduction in *Smg1* relative expression compared with *Smg1*$^{+/+}$ mice, and both showed one peak in the dissociation curve, indicating generation of a single PCR product. The *Smg1* relative expression in the *Smg1*$^{-/-}$ mice was also low; however, it showed multiple peaks with low amplitude in the dissociation curve, indicating weak binding of primers probably due to an absence of WT *Smg1* template in these samples.

Genotyping from Genomic DNA. PCR reactions were performed in an ABI 2720 thermal cycler (Applied Biosystems). To detect the SMG1 WT allele, the reaction mix comprised 1× LongAmp buffer (New England Biolabs), 0.25 mM $MgSO_4$ (Sigma), 0.25 mM dNTPs (Invitrogen), 1 M Betaine (Sigma), 1 μM forward primer (5′ CGAAGACTGGCTACTGTAAAG C 3′), 1 μM reverse primer (5′ AATTGTGAGGTGC CCAACACGAAT 3′), 1 unit of LongAmp Taq DNA polymerase (New England Biolabs), 50 ng of template DNA, and sterile water to 20 μL. Thermal cycling commenced with an initial 3-min denaturation at 95 °C, followed by 3 cycles of denaturation at 95 °C for 30 s, annealing at 63 °C for 30 s, and extension at 72 °C for 4 min; 3 cycles of denaturation at 95 °C for 30 s, annealing at 61 °C for 30 s, and extension at 72 °C for 4 min; 3 cycles of denaturation at 95 °C for 30 s, annealing at 59 °C for 30 s, and extension at 72 °C for 4 min; 3 cycles of denaturation at 95 °C for 30 s, annealing at 57 °C for 30 s, and extension at 72 °C for 4 min; and 35 cycles of denaturation at 95 °C for 30 s, annealing at 55 °C for 30 s, and extension at 72 °C for 4 min. A final extension was performed at 72 °C for 10 min. To detect the SMG1 Genetrap allele, the reaction mix comprised 1× LongAmp buffer (New England Biolabs), 0.25 mM dNTPs, 1 M Betaine, 1 μM forward primer (5′ TGGGGTAAAGGTGA GAGGGACAGG 3′), 1 μM reverse primer (5′ GTAATGGGATAG GTCACGTTGGTG 3′), 1 unit of LongAmp Taq DNA polymerase, 50 ng of template DNA, and sterile water to 20 μL. The thermal cycling condition was performed as described above. All PCR reactions were halted by bringing the temperature to 4 °C. SMG1 WT allele generated an ∼3-kb band, whereas SMG1 Genetrap allele generated a 1-kb band.

5′ RACE. 5′ RACE was performed using a FirstChoice RLM-RACE kit (Ambion) according to the manufacturer's instructions. Cassette-specific primers used for the nested PCR assay were outer primer (5′ GACGACGACAGTATCGGCCTCAG 3′) and inner primer (5′ TTTTCCCA GTCACGACGTTGT 3′).

Southern Blotting. Genomic DNA (10 μg) from WT (T4K) and heterozygote (T3B) mice was digested overnight with appropriate restriction enzymes and separated on 1% tris acetate EDTA agarose gels. DNA was Southern blotted onto an Amersham Hybond-XL positively charged nylon membrane (GE Healthcare) overnight via capillary transfer in 0.4 N of NaOH. Radioactive probes for the detection of the Genetrap cassette and *Smg1* exon 4 were created using a Rediprime II Random Prime Labeling System (GE Healthcare) and 20 μCi (0.74 MBq) of [α-32P]-dCTP (PerkinElmer). Hybridizations were performed overnight at 42 °C in Ambion ULTRAHyb buffer (Life Technologies) according to the manufacturer's instructions. Membrane washes were performed at 65 °C in SSC buffer (2×, 0.1×, and 0.05×) plus 0.1% SDS. Membranes were exposed onto Super RX medical X-ray film (Fujifilm) at −80 °C.

Measuring Insulin-Like Growth Factor-1 Levels. Serum insulin-like growth factor-1 (IGF-1) was measured with the mouse/rat IGF-1 ELISA (catalog no. MG100; R&D Systems), as specified by the manufacturer.

Analysis of Body Mass Composition. *Smg1*$^{+/gt}$ and *Smg1*$^{+/+}$ mice were anesthetized, and blood was collected via cardiac puncture. Blood was clotted at room temperature and centrifuged to separate serum, which was then aspirated and frozen. Following blood collection, the mice were killed and lean mass (grams), fat mass (grams), and bone mineral density (grams per square centimeter) were determined by dual-energy X-ray absorptiometry (DEXA) using a PIXImus densitometer (GE Lunar). Mice were scanned with their limbs splayed apart to allow reproducible positioning in a prone position on the imaging tray. Quality control and calibration were carried out within 24 h before each scanning period using the phantom and procedures

supplied by GE Lunar. The precision of the machine was measured at a coefficient of variation of 2.3%.

Histological Analysis of Bones. Following DEXA, the left hind limb of mice was dissected, extraneous soft tissue was removed, and the limb was fixed in 4% paraformaldehyde at 4 °C overnight. The bones were then decalcified for 4 wk in 14% EDTA (Sigma), pH 7.2. Once decalcified, bones were processed for paraffin embedding using a Shandon Pathcenter Processor (Thermo Electron Corporation). Five-micrometer bone sections were then deparaffinized and rehydrated as previously described (1). Sections were stained with H&E, mounted, and analyzed as previously described (2).

Quantitative PCR and Analysis. For telomere analysis, the spleen, liver, lung, and thymus were isolated from the *Smg1*$^{+/gt}$ and WT adult mice at 9–12 mo of age. Genomic DNA from these tissues was homogenized and purified using a phenol/chloroform method. The telomere lengths from these organs were quantitated by real-time PCR as described previously (3). All other quantitative PCR assays were performed as described previously (4). An ABI 7900 sequence detection system with SDS version 1.9 software (Applied Biosystems) was used. Table S4 shows the sequences of primers used for quantitative PCR assays.

SMG1 Immunoprecipitation. Murine embryonic fibroblasts (MEFs) from *Smg1*$^{+/+}$ and *Smg1*$^{+/gt}$ mice were grown to confluency, harvested, and lysed in radioimmunoprecipitation assay (RIPA) buffer [50 mM Tris (pH 8), 150 mM NaCl, 0.5% deoxycholate, 1% Nonidet P-40, 0.1% SDS]. For tissues, 40 μg of tissue was homogenized in RIPA buffer. Protein concentration from lysates was determined, and 400–1,000 μg of protein was used for each immunoprecipitation. Lysates were precleared with protein G agarose beads for 2 h at 4 °C. Cleared lysates were then incubated with sheep anti-SMG1 antibody (5) overnight at 4 °C, and complexes were precipitated by incubating with protein G agarose for 90 min. Protein levels were then measured by Western blotting with rabbit anti-SMG1 (Bethyl Laboratories).

Cell Cycle Analysis. Asynchronous single cells were harvested and then fixed with 70% ethanol and stored at −20 °C for 24 h before analysis. Approximately 1×10^6 cells were incubated with 30 μg/mL propidium iodide mix (Sigma–Aldrich), and DNA content was determined using FACScan (Becton Dickinson). Data were analyzed with Modfit software (Verity Software House).

Hypoxia Experiment. *Smg1*$^{+/+}$ and *Smg1*$^{+/gt}$ immortalized MEFs were cultured under normoxic or hypoxic condition (1% O_2) for 6 h or 18 h and harvested in 150 μL Western lysis buffer. Hypoxia inducible factor-1α Western blot analysis was performed as described (6). Total Erk1/2 and pErk1/2 Western blot analyses of these samples were performed as described (7).

Reactive Oxygen Species Measurement in Splenocytes. Splenocytes were isolated from *Smg1*$^{+/+}$ and *Smg1*$^{+/gt}$ mice that were ∼9 mo of age and were cultured in 250 μM H_2O_2 or 10 μM Rotenone (Sigma) for 4 h or 24 h. Reactive oxygen species measurements of treated splenocytes were determined by preloading of 10 μM 2′,7′-dichlorodihydrofluorescein diacetate (DCFDA) (Molecular Probes) or 5 μM MitoSox (Molecular Probes) for 30 min at 37 °C and then analyzed on FACSCalibur (BD Biosciences) and CellQuest (BD Biosciences) instruments.

Immunofluorescence and Immunohistochemistry. A γH2AX (Millipore) and ionizing radiation-induced DNA damage repair response was performed as described previously (8). γH2AX staining was performed on hyperplasia spleen sections, with 0.05% trypsin epitope retrieval at 37 °C for 20 min. The primary antibody was diluted 1:100 in blocking solution (20% FCS, 2% BSA, 0.2% Triton-X 100 in PBS) and incubated at 4 °C overnight. Assessment of 8-oxo-2′-deoxyguanosine (Trevigen) immunofluorescence for oxidative stress on hyperplasia spleen sections was performed according to the manufacturer's instructions. Oxidative stress was also analyzed on hyperplasia spleen sections via ProK epitope retrieval at 37 °C for 20 min and stained at 4 °C overnight with 4-hydroxynonenal (Chemicon) diluted 1:100 in blocking solution (10% FCS, 2% BSA, 0.2% Triton X in PBS). Sections were stained with appropriate secondary antibodies and imaged using a Zeiss AxioSkop fluorescence microscope. MPO (Abnova), B220/CD45R (Molecular Probes), CD3 (Biocare Medical), and Bcl2 (N-19; Santa Cruz Biotechnology) immunohistochemistry was performed by the QIMR histological service.

Stress Granule Formation. Stress granule formation was induced in *Smg1*$^{+/gt}$ and *Smg1*$^{+/+}$ MEFs by incubation with 1 mM sodium arsenite for 1 h. Stress granule formation was measured by immunofluorescence as described previously (9).

Computed Tomography Scan of Teeth. Computed tomography was used to scan the skulls of *Smg1* mice with deformed teeth as well as normal controls. Animals were placed in the second bed position and scanned using an Inveon PET/CT scanner (Siemens). Images were acquired using Inveon Acquisition Workplace software (Siemens) with the following settings: 360° rotation with 180 rotation steps, 20 calibrations, 11.8 pixels calibrating center offset, medium magnification (width = 40.6 mm, height = 60.8 mm), and 270-ms exposure with 4× binning. The X-ray tube was set at 80 kV and 500 μA. Images were reconstructed using Inveon Reconstruction Workplace software (Siemens) and multimodal 3D visualization of computed tomography mouse bone (calibrated) with default settings: bilinear interpolation, Shepp–Logan reconstruction filter, a down-sample factor of 1, and a final volume size of 512 × 512 voxels.

Craniofacial Measurements. Digital imaging and communications in medicine (DICOM) data were imported into Ezy3D software (Vatech). Longitudinal and angular craniofacial measurements were undertaken as described by Ramirez-Yañez et al. (10). Statistical comparisons were undertaken using a Student *t* test with $P < 0.05$.

1. Chang MK, et al. (2008) Osteal tissue macrophages are intercalated throughout human and mouse bone lining tissues and regulate osteoblast function in vitro and in vivo. *J Immunol* 181(2):1232–1244.
2. Alexander KA, et al. (2011) Osteal macrophages promote in vivo intramembranous bone healing in a mouse tibial injury model. *J Bone Miner Res* 26(7):1517–1532.
3. O'Callaghan N, Dhillon V, Thomas P, Fenech M (2008) A quantitative real-time PCR method for absolute telomere length. *Biotechniques* 44(6):807–809.
4. Roberts TL, et al. (2009) HIN-200 proteins regulate caspase activation in response to foreign cytoplasmic DNA. *Science* 323(5917):1057–1060.
5. Brown JA, et al. (2011) A novel role for hSMG-1 in stress granule formation. *Mol Cell Biol* 31(22):4417–4429.
6. Lévesque JP, et al. (2007) Hematopoietic progenitor cell mobilization results in hypoxia with increased hypoxia-inducible transcription factor-1 alpha and vascular endothelial growth factor A in bone marrow. *Stem Cells* 25(8):1954–1965.
7. Chen RQ, et al. (2009) Kinome siRNA screen identifies SMG-1 as a negative regulator of hypoxia-inducible factor-1alpha in hypoxia. *J Biol Chem* 284(25):16752–16758.
8. Harris JL, et al. (2009) Aprataxin, poly-ADP ribose polymerase 1 (PARP-1) and apurinic endonuclease 1 (APE1) function together to protect the genome against oxidative damage. *Hum Mol Genet* 18(21):4102–4117.
9. Brown JA, et al. (2011) A novel role for hSMG-1 in stress granule formation. *Mol Cell Biol* 31(22):4417–4429.
10. Ramirez-Yañez GO, Smid JR, Young WG, Waters MJ (2005) Influence of growth hormone on the craniofacial complex of transgenic mice. *Eur J Orthod* 27(5):494–500.

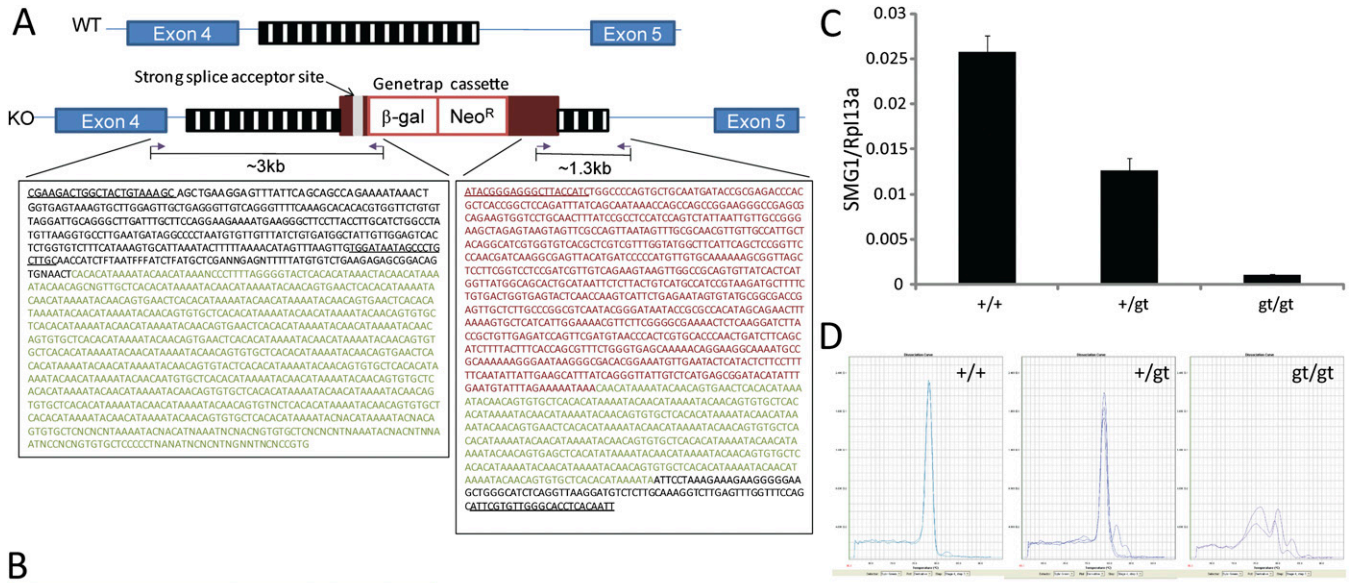

B

GCGGATCCGAACACTGCGTTTGCTGGCTTTGATGGAACAGATCGCAGTGTCGGCGGCGGCCGGTTCAGGCGGCGACTCGCGCTTCTTCGGGCGGCGGCGCTTGGCCATGTCGTGTC
GGGGAAGGTAATGAGCCGCAGAGCCCCGGGGTCTCGGCTGAGCAGCGGCGGCGGCGGCACCAAGTACCCGCGGAGCTGGAATGACTGGCAACCCAGAACTGATAGTGCATCAGCCG
ACCCAGATACTTTAAAATACTCCTCATCTAGAGATAGGGGTGTTTCTTCCTCTTATGGACTGCAACCTTCAAATTCAGCTGTGGTGTCTCGGCAAAGGCACGATGATACCAGAGGC
CATGCTGACATACAGAATGACGAAAAGGGTGGCTACAGTGTCAATGGAGGATCTGGGGAAAATACTTATGGTCGGAAGTCGTTGGGGCAAGAGCTGAGGATTAACAATGTGACCAG
CCCTGAGTTTACCAGTGTTCAGCATGGCAGTCGTGCATTAGCCACCAAAGACATGAGGAAATCACAGGAGCGATCGATGTCGTACTCTGATGAGTCTCGACTGTCGAATCTTCTTC
GGAGGATCACCCGGGAAGATGACAGAGACCGAAGACTGGCTACTGTAAAGCAGCTGAAGGAGTTTATTCAGCAGCCAGAAAATAAACTGGTCCCAGGTCCCGAAAACCAAAGAANA
AGAACGCAGATCGCATCGATAACTTCGTATAGCATACATTATACGAAGTTATCGCAGATCTGGACTCTANAGGNANTCCCGTCGTTTTTACAACGTCNTGACTGGGAAA

Fig. S1. Genotyping of embryos from *Smg1*$^{+/gt}$ × *Smg1*$^{+/gt}$ timed matings. (*A*) Schematic shows the insertion of the Genetrap cassette into intron 4 of the *Smg1* gene. Sections of the cassette and surrounding genomic DNA were sequenced to map the insertion site. Underlined sections indicate primers used for PCR from cDNA and sequencing, bold indicates the exon sequence, green text indicates the repeat region, black text indicates other intron sequence, and maroon text indicates the cassette sequence. (*B*) 5′ RACE product was excised from the agarose gel and directly sequenced. The highlighted yellow region indicates the commercial 5′ RACE inner primer, purple text indicates the 5′ UTR, alternating bold and regular font shows exons of *Smg1* gene, the underlined sequence indicates the Genetrap cassette, and red text indicates the inner cassette specific primer binding site. (*C*) Level of *Smg1* transcript in the embryo was determined by real-time PCR and expressed relative to the level of the control gene *rpl13a*. Data shown are examples of the data for individual embryos. Bars show the average expression level and range of replicate measurements. (*D*) Dissociation curves for the data shown in *C*. Both *Smg1*$^{+/+}$ and $^{+/gt}$ samples show production of a single dominant PCR product, but no specific amplification was observed in samples from the *Smg1*$^{gt/gt}$ embryos.

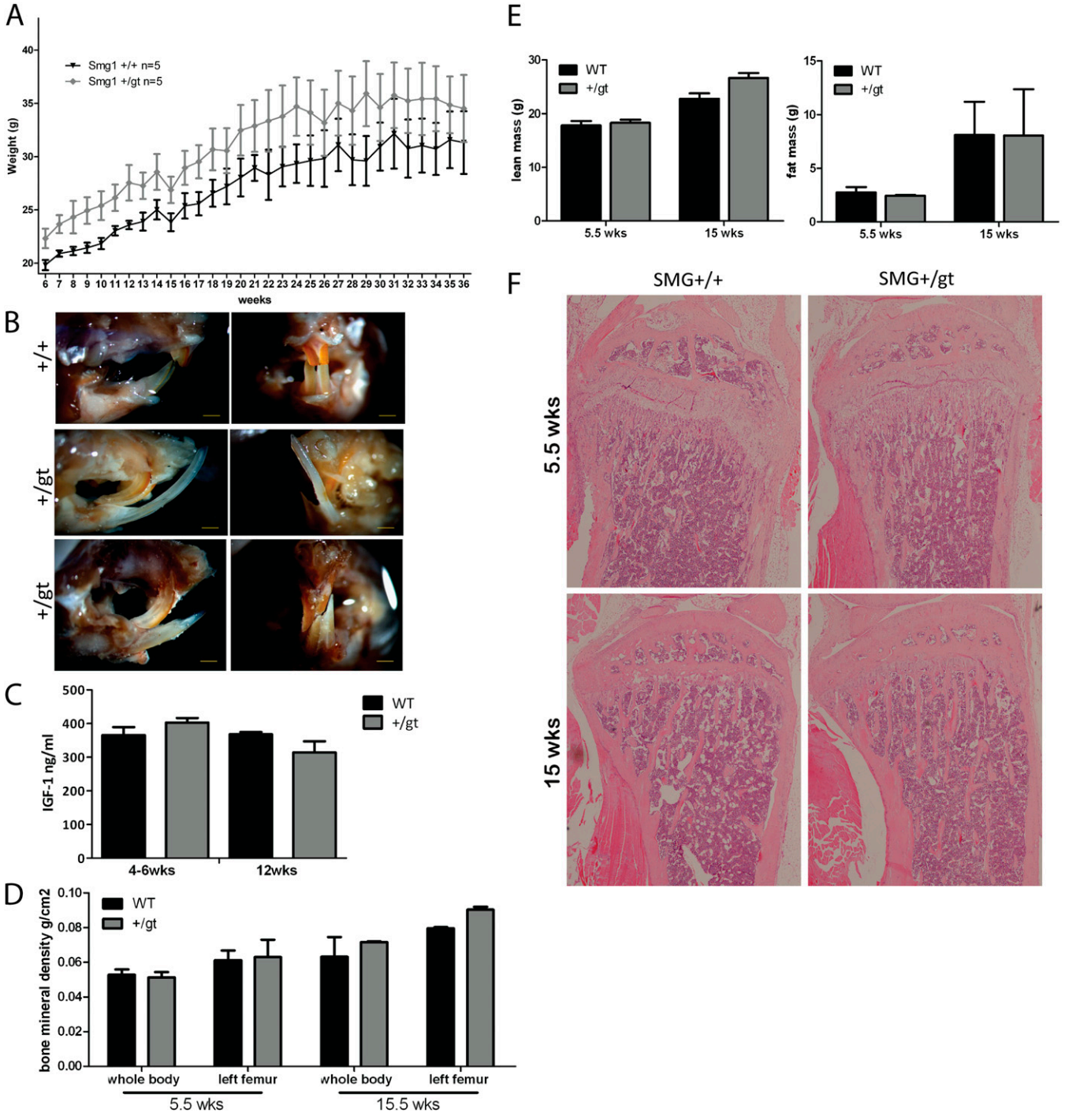

Fig. S2. *Smg1*$^{+/gt}$ mice show sporadic abnormalities in tooth development and growth. (*A*) Small cohort of *Smg1*$^{+/gt}$ and *Smg1*$^{+/+}$ littermates ($n = 5$) were weighed weekly from 6 wk to 6 mo of age. *Smg1*$^{+/gt}$ mice were significantly larger (Student *t* test, $P < 0.001$) than their *Smg1*$^{+/+}$ littermates. Data are expressed as mean ± SEM. (*B*) Small percentage of *Smg1*$^{+/gt}$ mice showed abnormal tooth development as pictured. (Scale bar = 1 mm.) (*C*) Because a percentage of *Smg1*$^{+/gt}$ mice were substantially larger than their *Smg1*$^{+/+}$ littermates, serum IGF-1 levels were measured by ELISA from six pairs of *Smg1*$^{+/gt}$ and *Smg1*$^{+/+}$ littermates. Data are expressed as mean ± SEM. (*D* and *E*) Two pairs of *Smg1*$^{+/gt}$ and *Smg1*$^{+/+}$ mice, each at 5.5 and 15.5 wk of age, were analyzed to determine bone mineral density and lean and fat mass. Data shown are pooled data expressed as mean ± SEM. (*F*) Bones from the mice analyzed in *C* and *D* were fixed, decalcified, and embedded, and bone structure was analyzed by H&E staining. No significant difference was seen between *Smg1*$^{+/gt}$ and *Smg1*$^{+/+}$ mice during the growth phase (5.5 wk) or after the growth phase (15.5 wk). Images were scanned at 4× magnification.

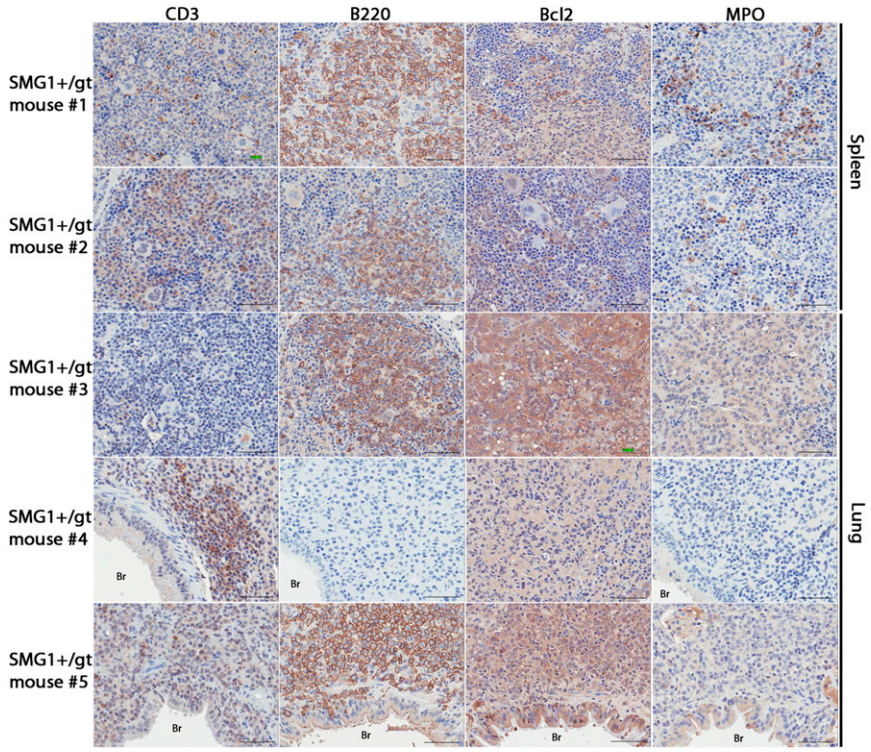

Fig. S3. Characterization of lymphomas from *Smg1*$^{+/gt}$ mice. Lymphoma samples from *Smg1*$^{+/gt}$ mice were further analyzed by immunohistochemical staining. Expression of CD3, B220, Bcl2, and myeloperoxidase (MPO) was determined for each lymphoma sample as indicated by brown staining. The majority of lymphomas stained positive for B220 and Bcl2, indicating that they are representative of non-Hodgkin lymphoma of follicular cell origin. (Scale bar = 100 μM.)

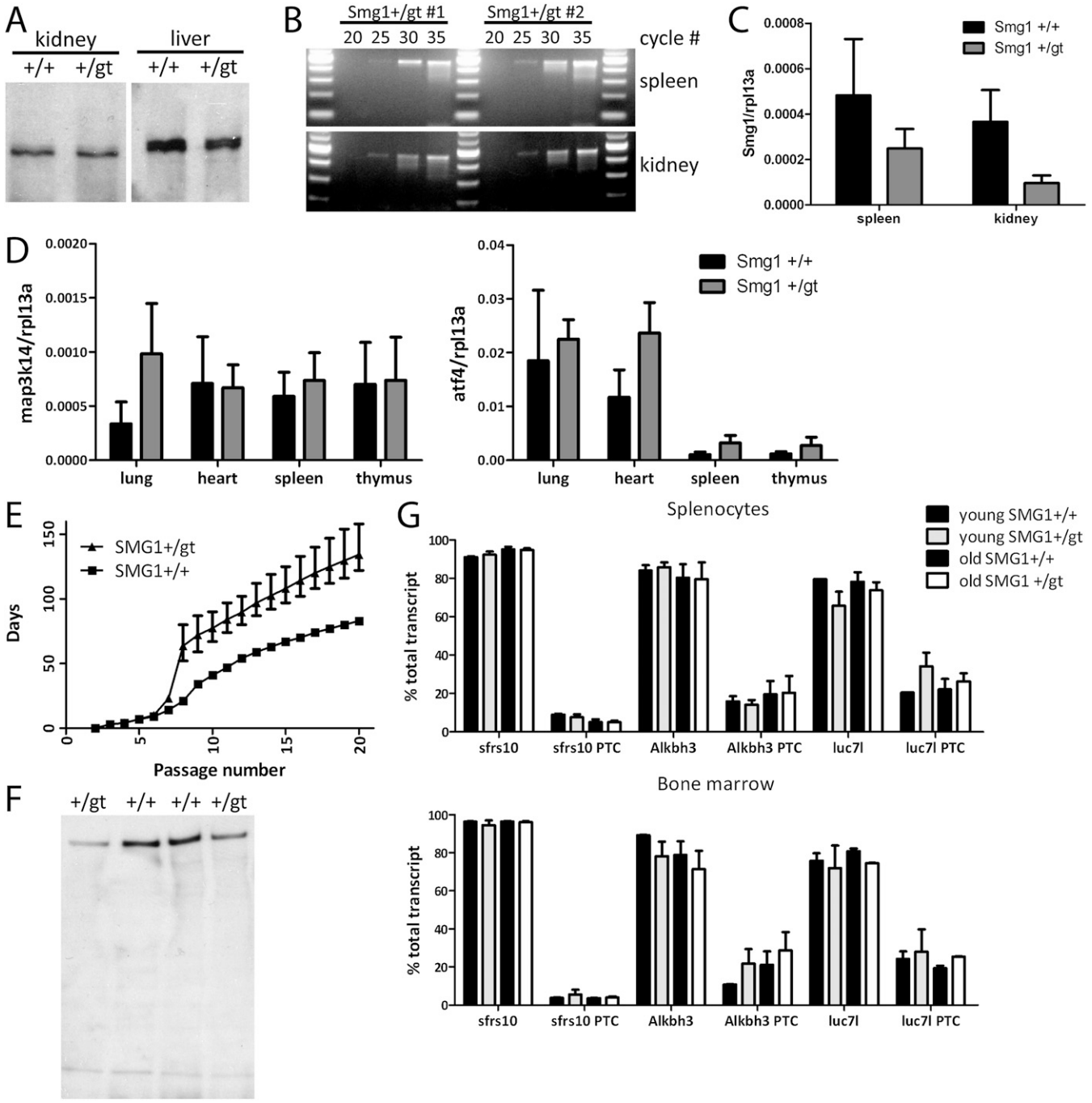

Fig. S4. *Smg1*$^{+/gt}$ mice do not show defects in nonsense-mediated decay (NMD). (*A*) SMG1 immunoprecipitation analyses were performed with sheep anti-SMG1 antibody on equal amounts of protein extract from *Smg1*$^{+/gt}$ and *Smg1*$^{+/+}$ samples from the kidney and liver. The level of SMG1 in the extracts was then determined by Western blotting. (*B*) Semiquantitative PCR assay was performed on cDNA from the kidney and spleen. Conditions were as described for genotyping from RNA in *SI Materials and Methods*. Samples were taken at the indicated cycle numbers and analyzed on agarose gels. (*C*) Levels of endogenous *Smg1* transcript were measured by real-time PCR assay and expressed relative to control transcript *rpl13a*. Data are pooled from four independent pairs of *Smg1*$^{+/gt}$ and *Smg1*$^{+/+}$ mice; bars show the average, and error bars show the SE. (*D*) Levels of endogenous NMD target transcripts were measured in tissues showing particularly low levels of SMG1 protein. Transcript levels were measured by real-time PCR assay and expressed relative to control transcript *rpl13a*. Data shown are pooled from five independent pairs of *Smg1*$^{+/gt}$ and *Smg1*$^{+/+}$ mice; bars show the average, and error bars show the SE. (*E*) Immortalized murine embryonic fibroblasts (MEFs) were crisis-derived by continuous passaging in tissue culture. Data shown are from a representative litter of embryos; points show the average day for each passage, and error bars show the range of days. MEFs from *Smg1*$^{+/gt}$ mice took longer to come through the crisis stage of immortalization than MEFs from *Smg1*$^{+/+}$ littermates. (*F*) SMG1 immunoprecipitation analyses were performed with sheep anti-SMG1 antibody on equal amounts of protein extract from *Smg1*$^{+/gt}$ and *Smg1*$^{+/+}$ MEFs. The level of SMG1 in the extracts was then determined by Western blotting with rabbit anti-SMG1 antibody. (*G*) Level of NMD-regulated splice variants was determined in splenocytes and bone marrow from young (3 mo) and older (9 mo) *Smg1*$^{+/gt}$ and *Smg1*$^{+/+}$ mice. The assay was performed as described for Fig. 3C. Data shown are pooled from two pairs of mice analyzed in independent experiments. Data are expressed as mean ± SEM.

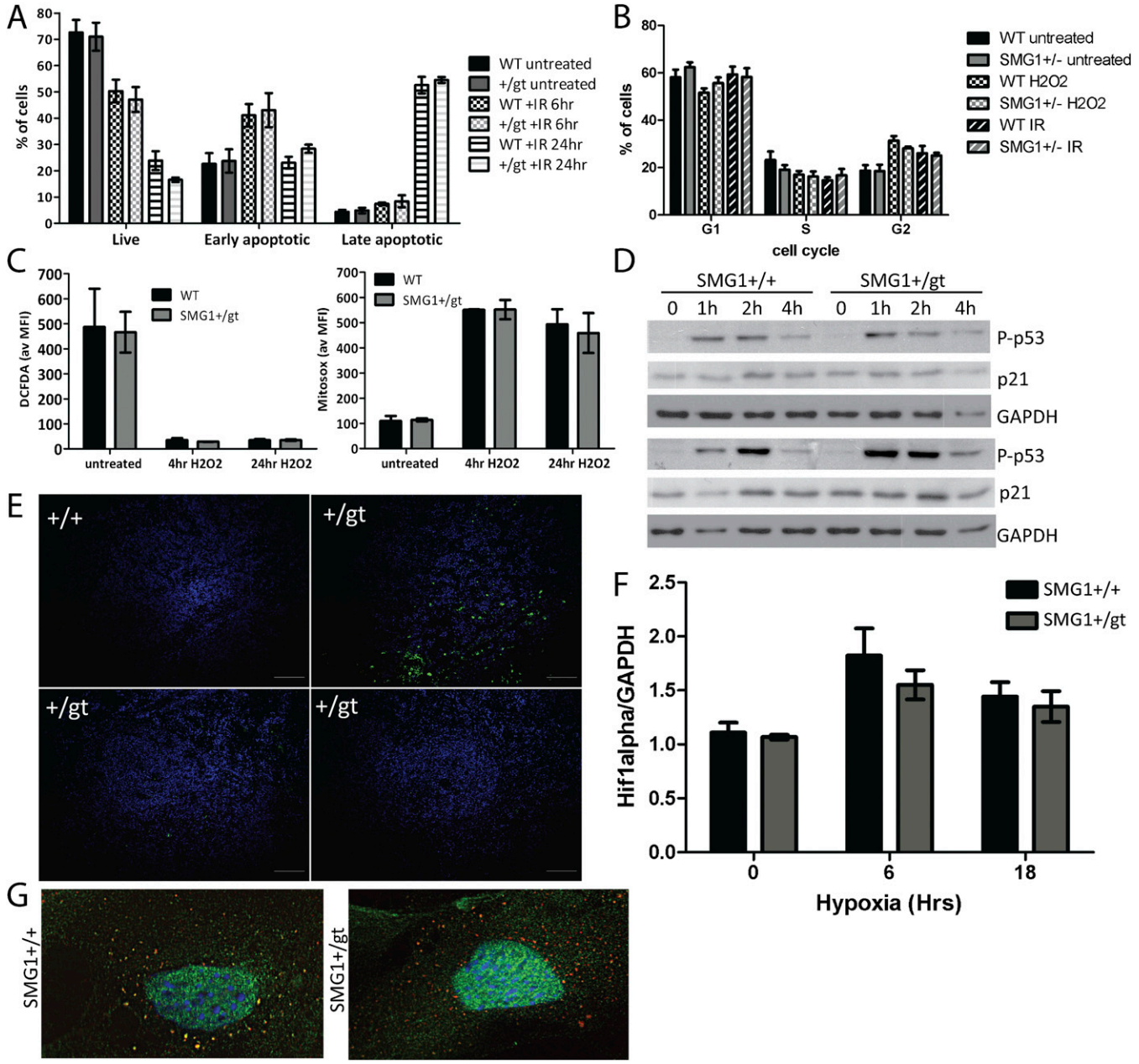

Fig. S5. *Smg1*$^{+/gt}$ mice do not show defects in DNA damage responses. (*A* and *B*) MEFs from *Smg1*$^{+/gt}$ and *Smg1*$^{+/+}$ littermates were treated with either 5-Gy ionizing radiation (IR) or 100 μM H_2O_2 for 24 h and were analyzed by flow cytometry for cell cycle progression and apoptosis. Data shown are pooled from three independent experiments. Data are expressed as mean ± SEM. (*A*) Apoptosis was measured by Annexin V expression and permeability to propidium iodide. (*B*) Cell cycle progression was determined by propidium iodide staining. Flow cytometry profiles were analyzed with ModFit software, and the percentage of cells in each phase of the cell cycle was determined. (*C*) Reactive oxygen species (ROS) production in response to H_2O_2 treatment. Splenocytes from *Smg1*$^{+/gt}$ and *Smg1*$^{+/+}$ mice were treated with 250 μM H_2O_2 for the indicated times. ROS production was determined by preloading with 10 μM 2′,7′-dichlorodihydrofluorescein diacetate (DCFDA) for cytosolic ROS or 5 μM MitoSox for mitochondrial ROS for 30 min at 37 °C before analysis by flow cytometry. DCFDA fluorescence decreases in the presence of ROS, whereas MitoSox fluorescence increases on ROS production. Data are pooled from three pairs of mice and are expressed as mean ± SEM. MFI, mean fluorescence intensity. (*D*) MEFs from *Smg1*$^{+/gt}$ or *Smg1*$^{+/+}$ mice were treated with 5 Gy IR and then harvested for protein extracts at the indicated time points. Levels of Ser18-phosphorylated p53 and total p21 were measured by Western blotting. GAPDH was measured as a loading control. (*E*) Tissues were formalin-fixed and embedded, and then stained with γH2AX antibody and DAPI to show nuclei. Tissues from *Smg1*$^{+/gt}$ mice with hyperplasia were compared with those from *Smg1*$^{+/+}$ mice of a similar age. (Scale bar = 100μM.) (*F*) MEFs from *Smg1*$^{+/gt}$ or *Smg1*$^{+/+}$ mice were placed in a hypoxic chamber for the indicated period of time. Cells were then rapidly lysed to generate protein extracts, and the level of hypoxia inducible factor-1α (HIF-1α) was determined by Western blotting, followed by densitometry. Data shown are pooled from three independent sets of MEFs. Data are expressed as mean ± SEM. (*G*) MEFs from *Smg1*$^{+/gt}$ and *Smg1*$^{+/+}$ mice were treated with 1 mM sodium arsenite for 1 h. Cells were then fixed and immunostained for SMG1 (green) and eiF4G (red). DAPI was used to stain nuclei. Images were taken on a Deltavision microscope (GE Healthcare) using a 60× oil immersion objective. No difference in stress granule formation was observed between the cell lines.

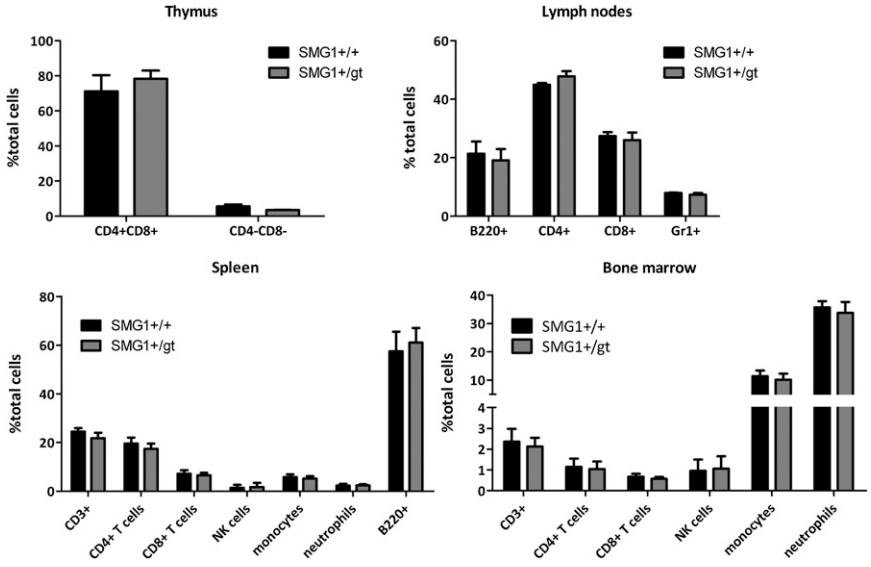

Fig. S6. Cellular composition of hematopoietic tissues in healthy *Smg1*$^{+/gt}$ and *Smg1*$^{+/+}$ mice. Tissues were harvested for *Smg1*$^{+/gt}$ and *Smg1*$^{+/+}$ mice, single cell suspensions were prepared, and cell surface marker expression was determined by flow cytometry. (*Upper*) Thymus and lymph nodes from young mice (6–8 wk) were analyzed for double-positive and double-negative T cells, B cells (B220^{+}), CD4^{+} and CD8^{+} T cells, and granulocytes (Gr-1^{+}). Data shown are pooled from three independent experiments. Data are expressed as mean ± SEM. (*Lower*) Cellular composition of the spleen and bone marrow of mice aged 6 wk to 9 mo for total (CD3^{+}) and CD4^{+} and CD8^{+} T cells, B cells (B220^{+}), natural killer (NK) cells, monocytes, and neutrophils. Data presented are pooled from all analyzed mice (three pairs for B220 and four pairs for other stains). Data are expressed as mean ± SEM.

Table S1. Craniofacial measurements of *Smg1*$^{+/gt}$ and *Smg1*$^{+/+}$ mice

			Longitudinal measurements, mm							Angular measurements, °			
Age, d	Sex	Genotype	A-Po	N-Mu	Ml-Pg	Co-Go	Go-Pg	Upper incisor	Lower incisor	AN/Nba	BuMu/Nba	GoPg/Nba	CoGo/GoPg
245	Female	*Smg1*$^{+/gt}$	20.9	5	3.9	5.3	8.1	12.4	12	117.9	41.1	44.5	101.3
69	Female	*Smg1*$^{+/gt}$	20.5	5.3	3	5.3	6.8	10.5	12.9	127	33	40.4	99.9
510	Male	*Smg1*$^{+/gt}$	25	6.6	4.9	6	7.1	11.5	14	127.3	35.1	43.4	106.9
499	Male	*Smg1*$^{+/gt}$	23.4	6.6	4.5	6.1	8.6	14.2	15.2	117.9	51.6	45.8	105.5
469	Male	*Smg1*$^{+/gt}$	22.6	6.7	4.5	5.6	7.4	8.7	15.1	121	29.5	51.1	110.5
509	Female	*Smg1*$^{+/+}$	21.6	5.6	4.1	5.6	6.3	9.2	10.4	124.7	33.8	64.8	105.6
560	Female	*Smg1*$^{+/+}$	22.2	5.5	4	5.1	7.1	7	9.1	127	42.1	62.4	102.9
839	Male	*Smg1*$^{+/+}$	24.5	6.2	4.5	5.7	7.3	15.7	19.3	133	37.6	50.3	119.9

Please see ref. 1 for a detailed description and illustration of the angles measured.

1. Ramirez-Yañez GO, Smid JR, Young WG, Waters MJ (2005) Influence of growth hormone on the craniofacial complex of transgenic mice. *Eur J Orthod* 27(5):494–500.

Table S2. Observations of mouse phenotype at autopsy

	Smg1$^{+/+}$ (total = 52)			*Smg1*$^{+/gt}$ (total = 137)		
Autopsy phenotypes	Average age, d	*n*	%	Average age, d	*n*	%
Enlarged uterus	644	4	12	529	8	13
Enlarged seminal vesicles	484	5	26	614	16	22
Discolored kidneys	408	5	10	525	32	24
Intestinal tumor	648	2	4	556	6	4
Stomach cysts	532	2	4	533	5	4
Enlarged spleen	587	9	18	550	49	36
Enlarged liver	537	8	16	626	35	26
Lung cysts/tumor	555	4	8	649	14	10

Table S3. Detailed pathology data on *Smg1*$^{+/gt}$ animals

Tissue	*Smg1*$^{+/gt}$ mice	No.	*Smg1*$^{+/+}$ mice	No.
Ovaries	Cyst (1), DLCL (1), normal (3)	5	Nodular luteinization of stroma cyst (1), normal (5)	6
Uterus	Lymphoma (2), DLCL (1), dilated vessels (1), normal (4)	8	Lymphoma (1), dilated endometrial gland (1), normal (4)	6
Testis	Normal (6)	6	Normal (4), dilated blood vessel (1)	5
Seminal vesicles	Dilated (3), DLCL (1), normal (6)	10	Normal (4), dilated (3)	7
Spleen	EMH (15), lymphoma (9), hyperplasia of white pulp (16), DLCL (11), spindle cell hemangioendothelioma (1), normal (15)	54	EMH (17), lymphoma (4), hyperplasia of white pulp (17), DLCL (1), congested red pulp (1), normal (13)	42
Liver	EMH (1), chronic inflammation (2), lymphoma (4), carcinoma (1), DLCL (6), steatosis (16), hepatitis (2), lymphoid infiltrates/foci (2), inflammation foci (2), centrilobular ischemic necrosis (1), cavernous hemangioma (1), normal (12)	48	EMH (1), chronic inflammation (2), lymphoma (1), DLCL (1), steatosis (6), inflammation foci (2), cavernous hemangioma (1), normal (20)	35
Kidney	Chronic inflammation (17), lymphoma (3), sclerosis (1), DLCL (4), chronic pyelonephritis (1), lymphoid infiltrate (2), normal (9)	38	Chronic inflammation (11), lymphoma (1), DLCL (1), chronic pyelonephritis (1), foci of inflammation (1), lymphoid infiltrate (1), normal (14)	30
Intestine	Cyst (1), plasmacytoid lymphoma (1), DLCL (3), blood clot (1), Chronic Inflammation (1), normal (3)	10	DLCL (1), normal (4)	5
Stomach	Hyperplastic polyp (1), DLCL (1), normal (1)	3	Dilated foveolae (1), hyperplastic polyp (2), gland cyst (1), normal (2)	5
Lung	Adenocarcinoma (7), chronic inflammation (14), congestion (1), pneumonia (1), DLCL (6), lymphoma (2), metastasis carcinoma (1), increased alveolar macrophages (1), normal (8)	39	Adenocarcinoma (1), chronic inflammation (4), DLCL (2), lymphoma (1), lymphoid infiltrate (5), fibrosis (6), normal (14)	33
Heart	DLCL (1), lymphoma (1), ischemic fibrosis (1), normal (22)	25	Lymphoma (1), normal (15)	16
Thymus	DLCL (9), lymphoma (3), thymoma (1), normal (13)	26	DLCL (1), lymphoma (2), hyperplasia (1), normal (17)	21
Head and neck	Adenocarcinoma (1), hyperplasia (1), DLCL (1), cyst (1)	4		0
Breast	Metastatic carcinoma (1), duct dilation (1)	2		0

Columns 3 and 5 indicate the number of slides analyzed for each particular tissue. For cases where the indicated pathologies (columns 2 and 4) equal more than the total slides, more than one type of pathology was detected in a single tissue, so more than one entry is present for the tissue. For entries where the total of columns 2 and 4 is less than 3 or 5, pathologies indicated were not detected in a tissue (and hence not recorded in this table), but the tissue was also not classed as normal by the pathologist. DLCL, diffuse large-cell lymphoma; EMH, extramedullary hematopoiesis; lymphoma, all non-DLCL lymphomas; No., number of sections analyzed.

Table S4. Primers used for real-time PCR analysis

Target gene	Forward primer 5′–3′	Reverse primer 5′–3′	Ref.
IL-1β	CAACCAACAAGTGATATTCTCCATG	GATCCACACTCTCCAGCTGCA	(1)
Csf-1	CCACCATCCACTTGTATGTCAAAGAT	CTCAACCACTGTCACCTCCTGT	(2)
Gas5	ATGCAGTGACTGCACCTTTGTTT	TTTTAACACAATATATCTGACACCATCTTC	(3)
rpl13a	GAGGTCGGGTGGAAGTACCA	TGCATCTTGGCCTTTTCCTT	(4)
IL-6	GATTGTATGAACAACGATGATGC	TGTTCTTCATGTACTCCAGGTAGC	
Smg1	GACCAGCCTACAATCCATCCT	CAAACTCTGCAACCACCCA	
Atf4	GAGTCTGAAGTCGGGACCAC	GATCGTCGGCTGGAACAC	(5)
Map3k14	ATCCAGTCTCTCAATGGCGAAC	CGAGCACTGAGATCAAAGGAAG	(5)

1. Roberts TL, et al. (2009) HIN-200 proteins regulate caspase activation in response to foreign cytoplasmic DNA. *Science* 323(5917):1057–1060.
2. Irvine KM, et al. (2006) A CSF-1 receptor kinase inhibitor targets effector functions and inhibits pro-inflammatory cytokine production from murine macrophage populations. *FASEB J* 20(11):1921–1923.
3. Chin PY, Macpherson AM, Thompson JG, Lane M, Robertson SA (2009) Stress response genes are suppressed in mouse preimplantation embryos by granulocyte-macrophage colony-stimulating factor (GM-CSF). *Hum Reprod* 24(12):2997–3009.
4. Mogal A, Abdulkadir SA (2006) Effects of Histone Deacetylase Inhibitor (HDACi); Trichostatin-A (TSA) on the expression of housekeeping genes. *Mol Cell Probes* 20(2):81–86.
5. Gardner LB (2008) Hypoxic inhibition of nonsense-mediated RNA decay regulates gene expression and the integrated stress response. *Mol Cell Biol* 28(11):3729–3741.

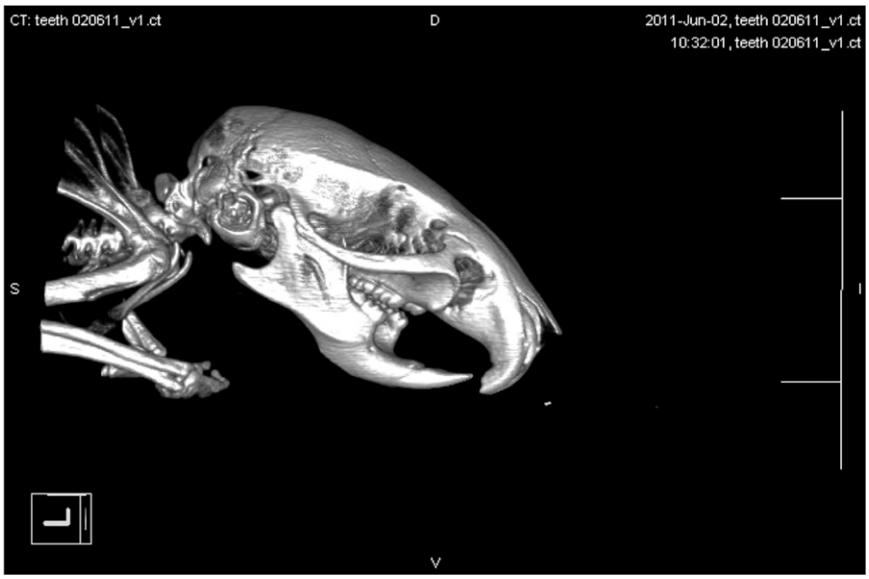

Movie S1. Computed tomography of the *Smg1*$^{+/+}$ mouse. This movie is representative of computed tomography scans of *Smg1*$^{+/+}$ mice. Animals were scanned using the Inveon PET/CT scanner. Scans were used to determine the craniofacial measurements in Table S1.

Movie S1

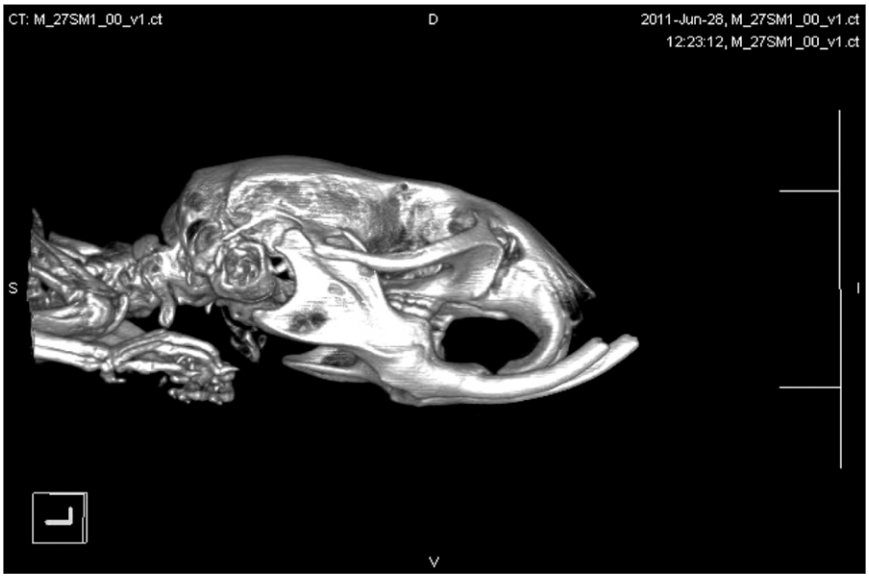

Movie S2. Computed tomography of *Smg1*$^{+/gt}$ mouse. This movie is representative of computed tomography scans of *Smg1*$^{+/gt}$ mice with deformed teeth. Animals were scanned using the Inveon PET/CT scanner. Scans were used to determine the craniofacial measurements in Table S1.

Movie S2